Global Scientific JOURNALS

GSJ: Volume 11, Issue 6, June 2023, Online: ISSN 2320-9186

www.globalscientificjournal.com

LEAD AMENDMENT IN PEROVSKITE SOLAR CELLS USING ETHYLENE VINYL ACETATE MODIFIED WITH DIAMMONIUM PHOSPHATE

[1]Chukwuwendu .J. AMAECHI, [2]Clement .N. OGBONDA & [3]Friday .B. SIGALO

[1]Department of Physics,

Ignatius Ajuru University of Education Rumuolumeni,

Rivers State, Nigeria.

chukwuendu.amaechi@iaue.edu.ng

[2]Department of Physics,

Ignatius Ajuru University of Education Rumuolumeni,

Rivers State, Nigeria.

Clement.ogbonda@iaue.edu.ng

[3]Department of Physics,

Rivers State University Port Harcourt,

Rivers State, Nigeria.

Sigalo.Friday@ust.edu.ng

KEYWORD: Amendment, band gap, ethylene vinyl acetate, layer, lead sequestration, optical properties, Perovskite, Solar cells

ABSTRACT

This research work explores the potential of phosphate-modified ethylene vinyl acetate films for lead amendment in perovskite solar cells. Perovskite solar cells are becoming increasingly popular due to their high efficiency, low cost, and easy fabrication. However, one of their main drawbacks is the use of lead (Pb) due to its toxicity. The first step in the study was to synthesize a series of phosphate-modified polymer films under various concentrations. Subsequently perovskite layer was deposited on the films and the films were soaked in water for 12 hours. The films were then subjected to atomic absorption spectroscopic characterization to assess their chemical properties. After the characterization tests, the films were used for lead amendment in perovskite solar cells to evaluate their performance. The results of this study indicated that phosphate-modified polymer films are promising candidates for lead amendment in perovskite solar cells due to their ability to capture over 99.9% of Pb leakage without compromising the performance and operation of the cells, which showed a power conversion of 6.0%, 3.2%, and 7.0% respectively. The active layers were characterized by UV-vis spectrophotometer, and the results showed excellent optical response and a narrow band gap of 1.7ev for the perovskite layer and 2.0eV for the TiO_2 layer.

1. INTRODUCTION

One of the most basic needs for surviving in today's technologically sophisticated civilization has proven to be energy. Due to escalating global energy consumption and pollution, traditional fossil fuels cannot support the viability of human progress. Nuclear power has been found to have safety and waste management issues despite its capacity to provide enormous amounts of electricity. The cornerstone for the advancement of human civilization is energy. Since the beginning of the first industrial revolution, when global energy consumption began to rise, it has become the primary driver behind technical advancement and innovation, which has fundamentally changed how people live today. The use of clean, renewable energy sources is now essential to the advancement of human civilization. Solar electricity is without a doubt one of the most promising new energy sources. Solar cells, which can transform sunlight into electricity, have long been a cornerstone of the renewable energy movement. Despite being very small on their own, individual cells can power

lights and replenish batteries when upgraded to modules. They may eventually act as the main energy source for buildings if they were positioned side by side. However, silicon-based solar cells currently cost more to build when compared to more traditional power sources. In this case, perovskite, a very effective substitute material, comes into play. This crystalline structure, when nestled into the center of a solar cell, turns light into energy just as well as silicon, but at a far cheaper cost. Perovskite-based solar cells may also be produced using rigid and flexible substrates, which makes them lighter, more flexible, and more inexpensive. To be useful in the real world, these prototypes must grow in size, effectiveness, and durability. The class of compounds known as perovskites gets their name from the mineral that exhibits its unique crystal structure. When utilized to make solar cells, they have shown promise for good performance and affordable manufacture. Since the first reports of ten percent efficiency solid-state perovskite solar cells utilizing methylammonium lead iodide ($CH_3NH_3PbI_3$) as the active component [7], perovskite solar cells have received a lot of interest. Since then, by optimizing both material and device architecture and by understanding the underlying mechanics of these devices, significant progress has been achieved in boosting efficiency (now over 20%) [9]. Despite the fact that long-term stability is necessary for practical applications, more research has been done on increasing device efficiency than on understanding deterioration and improving stability. Despite encouraging first results showing strong cell stability in the ambient environment over a 500-hour period [10], it is well-recognized that stability, particularly under light, is a severe concern in perovskite devices. Perovskite solar cells, made of organic-inorganic hybrid material have seen considerable and quick development during the past ten years. The market is still dominated by Si-based photovoltaic (PV) technology even though the power conversion efficiency of PSCs has grown from 3.8% to 25.8%, nearing that of commercial single crystalline Si solar cells. This is because scaling up PSCs, enhancing device stability, and lowering PSCs toxicity are difficult tasks that stand in the way of commercializing perovskite PV technology. It is particularly challenging for PSCs to enter the

market because of the toxicity caused by lead leakage [18]. PSC is the most promising material for tandem solar cells and building integrated photovoltaic devices because of its exceptional ability to modify bandgap within the range of 1.3 to over 3.0 eV through composition engineering [5]. Therefore, researchers are becoming more and more interested in creating and improving PVSCs in order to enhance their functionality and enable their wider acceptance as a clean and effective substitute for conventional fossil energy sources.

2. MATERIALS AND METHODS

2.1 Production of the Phosphate-Modified Polymer Films

The polymer used in the research work is ethylene vinyl acetate (EVA). It was prepared as follows;

Solution 1: 4g of EVA + 40ml of Toluene. (Toluene is used as a solvent because EVA has a semi-crystalline structure, and it's composed of an amorphous and crystalline part. Eva is not soluble in water but soluble in toluene).

10g of (DAP) diammonium phosphate $(NH_4)_2(HPO_4)$ was dissolved in 20 ml of water and incorporated into the polymers at different proportions as seen below.

Sample E1: EVA + DAP of 1g

Sample E2: EVA + DAP of 0.6g

Sample E3: EVA + DAP of 0.2g

All the samples of the films were deposited by the doctor-blading method, and the thickness of the spacer (i.e. a sticky tape used for the separation of samples) was 170 microns. The deposited polymer films were cut into sizes of 1cm X 1cm for effective covering of the cells. Perovskite was deposited using the spray pyrolysis method on six samples, and all the samples of the polymer films was used to laminate each of the six FTO glass substrates at a controlled temperature. They were each soaked in 5 ml of water in a sample bottle for 12 hours. The phosphate modified polymer

films/FTO substrates with perovskite, were removed from the sample bottles afterwards, and the water was subjected to further investigation using atomic absorption spectrophotometer. This was done to ascertain which of the films had excellent encapsulation ability to trap the lead in the perovskite material from leaching into the water.

2.2 Preparation of the Perovskite Material

The chemicals used for the perovskite layer are Formamidinium Iodide (FAI, Sigma-Aldrich Chemie GmbH Germany), Methylammonium bromide (MABr, Sigma-Aldrich Chemie GmbH Germany), Lead iodide (PbI_2, Sigma-Aldrich Chemie GmbH Germany), Lead bromide (PbBr2, Sigma-Aldrich Chemie GmbH Germany) and they were dissolved in a mixture of N,N-Dimethylformamid (DMF, Aldrich) and Dimethyl sulfoxide (DMSO, Aldrich) with a volume ratio of 4:1. The molar ratio for the FAI:PbI_2:MABr:$PbBr_2$ perovskite precursor solution was 1:1.1:0.2:0.2. For interfusion of the chemicals and solvents to a single solution, the molar concentrations for each constituent were increased by two. Before mixing, the iodide compounds (FAI+PbI_2) and the bromide compounds (MABr+$PbBr_2$) were dissolved with DMF: DMSO in separate vials. Then equal volume amount from $FAPbI_3$ and $MAPbBr_3$ was added together to get the wanted molar concentration. The colour of the solution was yellow, and the following reaction illustrates how perovskite is formed:

$$CH_3NH_3PbBr_2 + PbI_2 \longrightarrow CH_3NH_3Br_2PbI_3$$

2.3 Numbering of Samples

Four pieces of the FTO glass substrates were labelled as follows;

- **Cell 1** (Control perovskite),
- **Cell 2** (DAP + EVA 0.6g + perovskite),
- **Cell 3** (DAP + EVA 0.2g + perovskite),

2.4 Fabrication of the Perovskite Solar Cells

The manufacturing process for the perovskite solar cell followed the structure listed below;

- FTO
- FTO/compact (blocking layer) TiO2
- FTO/compact TiO2/mesoporous TiO2

- FTO/compact TiO2/mesoporous TiO2/perovskite
- FTO/compact TiO2/mesoporous TiO2/perovskite/elcocarb/
- FTO/compact TiO2/mesoporous TiO2/perovskite/elcocarb/Cu

The procedure steps for deposition of the materials are seen below.

1. Cleaning: The FTO/glass substrates need to be cleaned before the different layer dispositions can commence because even a small dust particle on the surface will affect the performance of the final cell.
2. Compact (blocking layer) preparation; the blocking layer of the FTO glass substrates for the samples was prepared by electrospinning and calcination from the precursor of a total volume of 40ml, which has a concentration of 0.1M of titanium isopropoxide, 0.4M of acetylacetone and methanol. Two drops of the originator solution were added onto the FTO glass substrates and spin-dried for 20 seconds. The black tapes were removed and the samples were annealed to 450^0C for 30 minutes [1]
3. The Titanium dioxide (TiO_2) electron transport layer was deposited onto the fluorine-doped tin oxide glass substrates by the chemical bath deposition method from a 70mm solution of titanium tetrachloride (Solaronix Titanium tetrachloride) outlining it on the active area. The samples were annealed at 70^0C. After annealing, the samples were allowed to cool down for 30 minutes.
4. The perovskite solution was spin-coated to obtain a thickness of 100-500 nm. In the second step, chlorobenzene (CB) was added when it was 15 seconds left of the spin-coating program. The chlorobenzene helps with the perovskite film formation by distributing the solution evenly and is a crucial step for obtaining high performance.

2.5 Atomic Absorption Characterization

Atomic Absorption Spectroscopy (AAS), was used to determine the concentration of Lead (Pb) (heavy metal) in the fabricated samples. The samples were each soaked in 5 ml of water in a sample bottle for 12 hours. The phosphate-modified polymer films/FTO substrates with perovskite, were removed from the sample bottles afterwards, and the water was read on the Thermo Scientific Atomic Absorption Spectrophotometer Model iCE 3000 Series at various wavelengths, at the Chemistry research section, Sheda Technological and Science Complex (SHETSCO) Kwali Abuja.

2.6 Optical Characterization of the Samples

A (UV 752) ultraviolet-visible-Near Infra-Red (UV-VIS-NI) spectrophotometer U.K was used to carry out the optical study of the cells at the wavelength interval of 230 nm to 1100 nm. A spectrophotometer is an instrument that measures the number of photons (the intensity of light) absorbed after it passes through the sample solution.

Absorbance values were obtained using the spectrophotometer and other optical properties like transmittance, reflectance, refractive index, absorption coefficient, extinction coefficient, and energy band gap were evaluated using the following equations;

The transmittance (T) of the cells was evaluated using Equation (1)

$$T = 10^{-A} \quad 1$$

Reflectance was obtained using equation (2)

$$R = 1 - (A + T) \quad 2$$

The refractive index of the cells was calculated using Equation (3)

$$\eta = \frac{(1+\sqrt{R})}{(1-\sqrt{R})} \quad .3$$

The absorption coefficient was calculated from absorbance spectra using Equation (4). Where *d* is the thickness and is measured in micrometers (μm), and *A* is the absorbance.

$$\alpha = \frac{2.303A}{d} \quad 4$$

The extinction coefficient was obtained using Equation 5

$$K = \frac{\alpha\lambda}{4\pi} \quad 5$$

Optical conductivity was estimated using Equation (6)

$$\sigma_o = \frac{\alpha\eta c}{4\pi} \quad 6$$

Where c is the speed of light.

The energy band gap was estimated using Tauc's model given in Equation (7)

$$(\alpha h\nu)^n = \beta(h\nu - E_g) \quad 7$$

Where α is the absorption coefficient, *h* is the Planck constant, ν is the photon's frequency, *E*g is the band gap energy and β is a constant. The *n* factor depends on the nature of the electron transition and is equal to ½ or 2 for the direct and indirect transition band gaps respectively.

3. RESULTS AND DISCUSSION

3.1 Result of Atomic Absorption Spectroscopy

Table 1: Result of Atomic Absorption Spectroscopy

SAMPLE ID	DATE SAMPLED	CONCENTRATION (mg/L)	TIME
Pb Control	3/23/2022	12.2542	2:03:53
Pb Ref	3/23/2022	-1.0330	2:05:53
Pb E1	3/23/2022	1.2338	2:11:57
Pb E2	3/23/2022	-0.9125	2:13:55

Pb E3	3/23/2022	-2.4051	2:15:49

Table 1 showed the concentration of Lead (Pb) in the samples. The Pb concentration level in the DAP - EVA films in the form of laminating tapes on the perovskite solar cells is presented in Table 1. The lead (Pb) concentrations in water for the devices are E1 = 1.2338 mg/L, E2 = - 0.9125 mg/L, and E3 = - 2.4051 mg/L. Remarkably, the Lead (Pb) concentration in water for the devices with DAP-EVA films remained below 12.2542 (Pb control) with a maximal value of only 1.2338 (E1). These results suggest a sequestration efficiency of 99.9% for samples E2, and E3 with values of (-0.9125, and – 2.4051) respectively, and less than the World Health Organization (WHO) value of 10µg/L for drinking water. The impact of the DAP+EVA laminating films on the photovoltaic performance of perovskite solar cells by using the device structure in two different amendment conditions: no amendment, amendment with DAP+EVA films showed that lead (Pb) absorbing film does not negatively impact both device power conversion efficiency (PCE), and stability of the PSCs. Finally, this work reports a chemical (Pb) absorbing laminating films capable of capturing over 99.9% Pb leakage from severely damaged perovskite solar cells.

3.2 Results of Optical characterization

Figure 1 - 4 showed the result of the optical properties for perovskite and the TiO_2. The graphical representations of the Absorption coefficient, reflectance, and optical bandgap for the perovskite and TiO_2 layers are presented below.

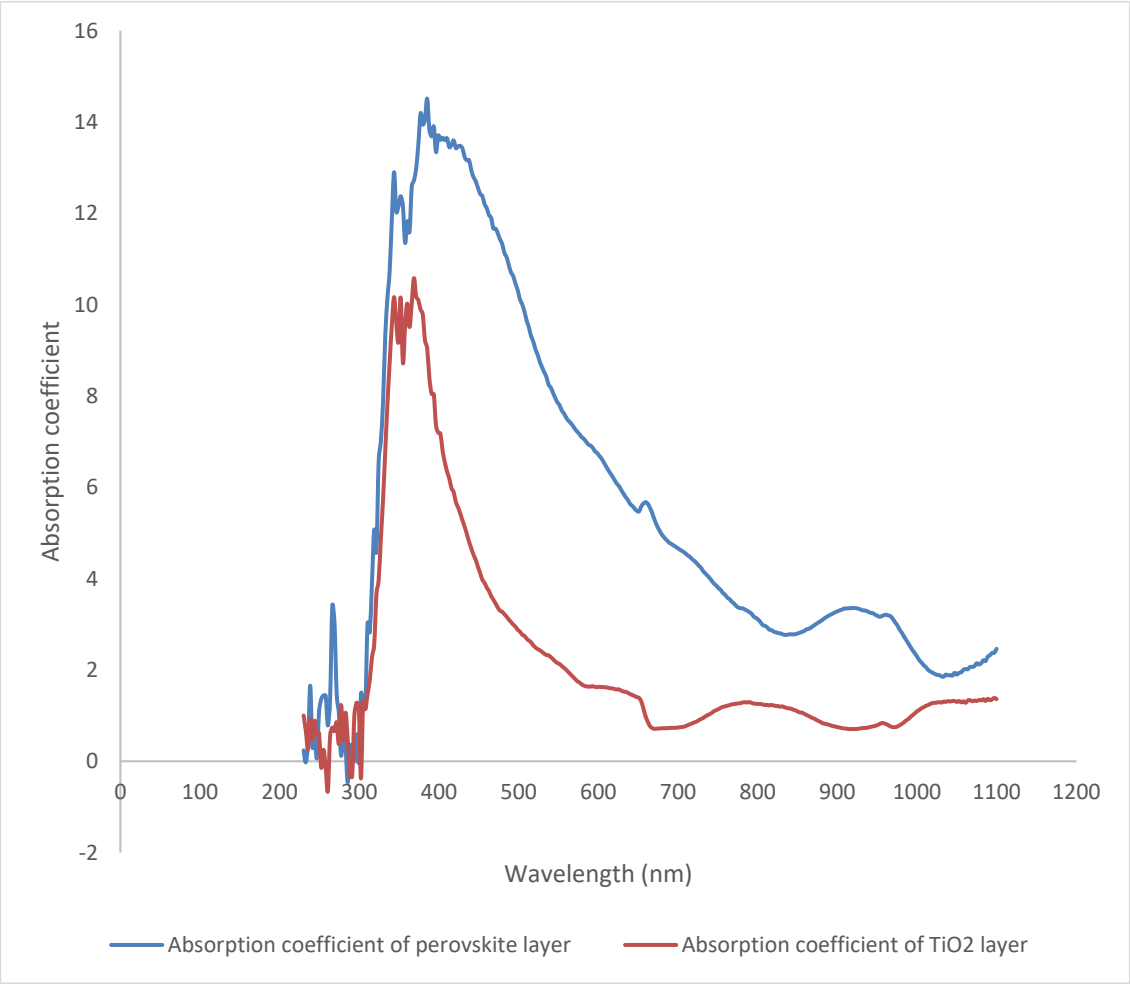

Figure 1: Uv-vis- Absorption Coefficient Spectra of Perovskite and TiO_2 Layer

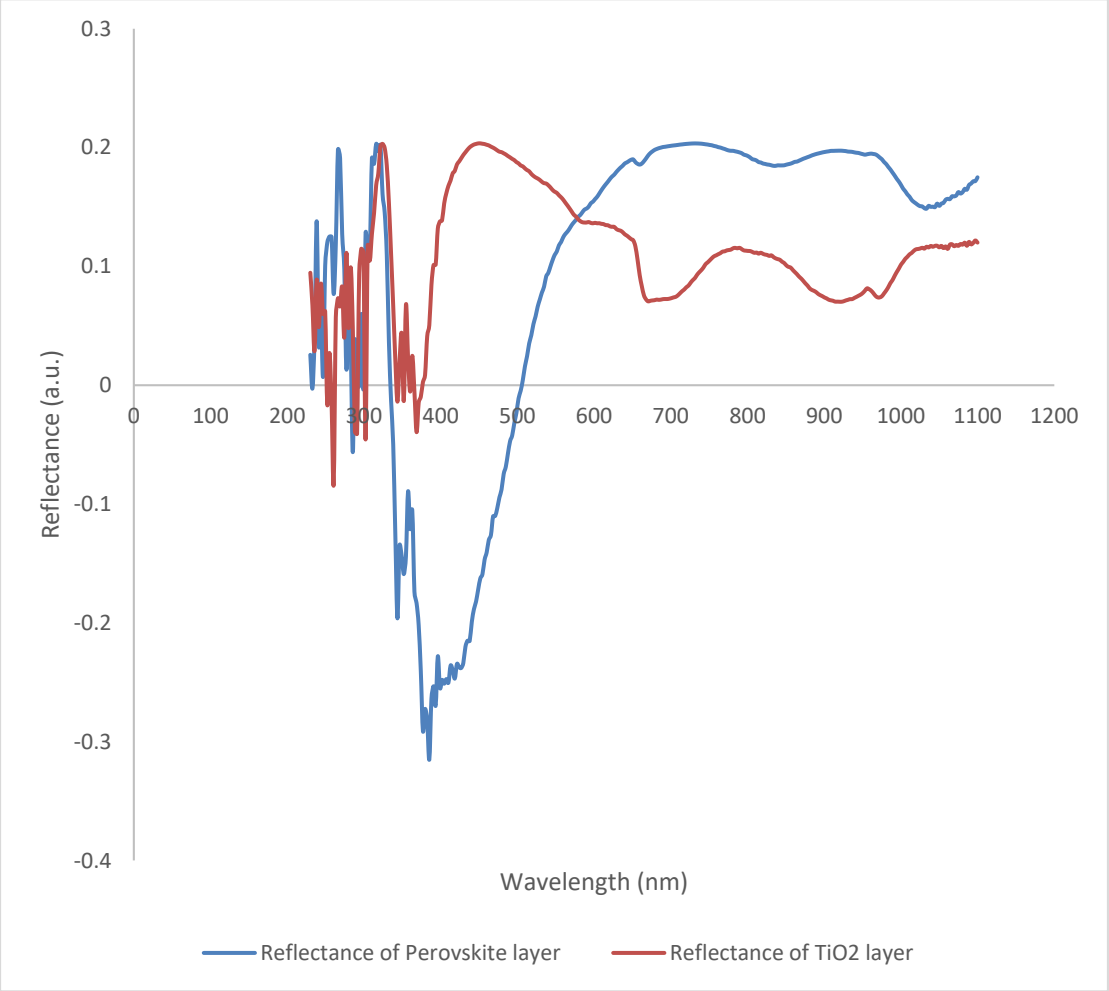

Figure 2: Uv-vis- Reflectance Spectra of Perovskite and TiO_2 Layer

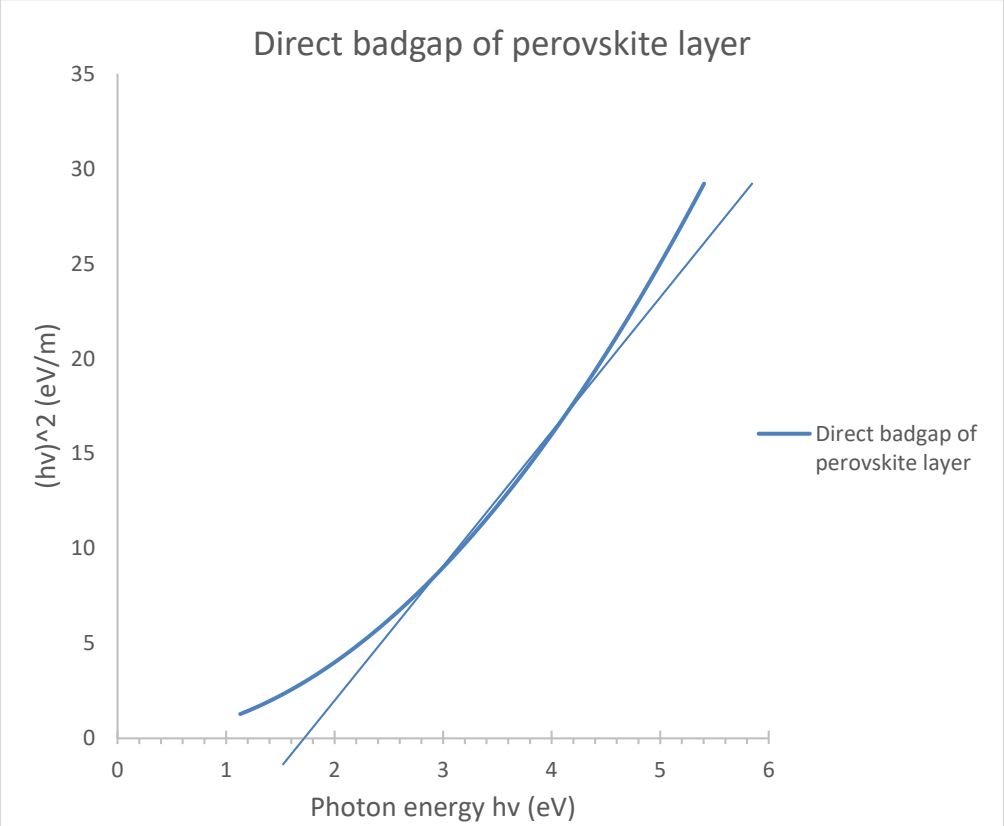

Figure 3: Direct Optical band gap of the Perovskite Layer

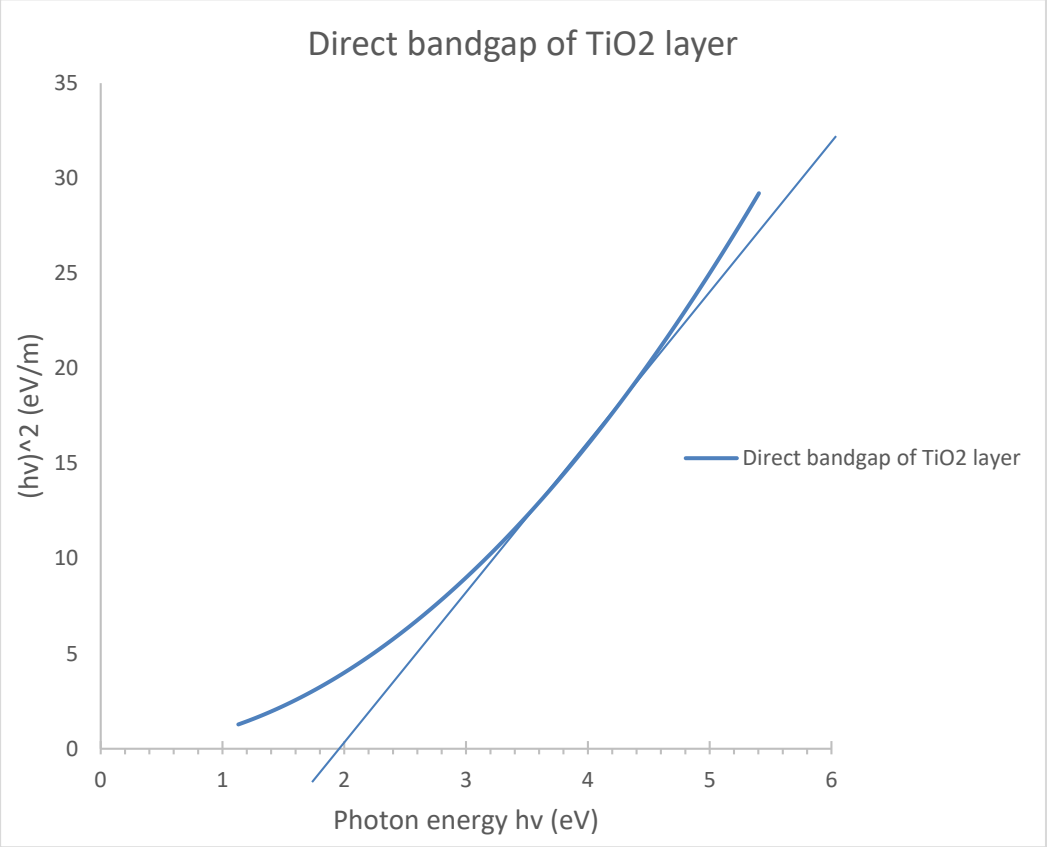

Figure 4: Direct Optical band gap of the TiO_2 Layer

Figure 1 showed the UV-vis absorption coefficient spectra of the perovskite and TiO_2 of the PSCs. The figure shows the presence of distinct absorption peaks in the visible region, the absorption peaks of the perovskite layers can be seen at about 350 nm to 500 nm. This indicates that the perovskite layer has higher absorption spectra wavelength within the visible spectrum. In the wavelength longer than 600nm, both films showed little absorption, allowing most of the incident light to reach other active layers. The absorption coefficient is the excitation of an electron from the valence band to the conduction band. The absorption coefficient was then used to estimate the direct optical energy band gap (Eg). Figure 2 - 4 shows the graphical representation of reflectance and direct optical band gap of the perovskite and TiO_2 layer. The direct optical band-gap for the perovskite layer was estimated to be 1.7eV by extrapolating the linear portion of the curve $(hv)^2$

against (hv), and also the direct optical band-gap for the TiO_2 layer was estimated to be 2.0 eV by extrapolating the linear portion of the curve $(hv)^2$ against (hv).

Photovoltaic parameters of the fabricated PSCs are; Voc was found to be 0.95, 0.90, 0.97, and 0.94 V and corresponding Isc values of 2.2, 1.4, 2.4, and 2.25 mA/cm^2 respectively for each of the perovskite solar cell (PSC) samples labelled Cell 1, Cell 2, Cell 3, and Cell 4. The fill factor was found to be 0.72, 0.634, 0.74, and 0.62 respectively for each of the PSCs samples. The power conversion efficiencies were 6.0% for cell 1, 3.2% for cell 2, 7.0% for cell 3, and 5.33% for cell 4.

CONCLUSION

Conclusively, four samples of perovskite solar cells were fabricated and their uv-vis absorbance spectra, transmittance spectra, reflectance spectra, refractive index, and absorption coefficient were determined using a (UV 752) ultraviolet-visible near infra-red (UV-VIS-NI) spectrophotometer. The lead (Pb) concentration level in the DAP-EVA films in the form of laminating tapes on the perovskite solar cells reports a chemical lead (Pb) absorbing laminating films capable of capturing over 99.9% Pb leakage from severely damaged perovskite solar cells. Meanwhile, this method follows general fabrication methods for perovskite solar cell without compromising device performance, thereby proffering a convenient method to ameliorate the potential lead leakage from damaged perovskite solar cell.

REFERENCES

[1] Amaechi, C. J., & Ogbonda, C. N. (2022). Roselle Plant Pigments as Natural Photosensitizers for Dye-Sensitized Solar Cells: The Effect of Tin Oxide Blocking Layer on the Photoelectric Properties. *Journal of Mathematical Sciences & Computational Mathematics*, *3*(4), 564-573.

[2] Ahn, K. S., Yan, Y., Lee, S. H., Deutsch, T., Turner, J., Tracy, C. E., ... & Al-Jassim, M. (2007). Photoelectrochemical properties of N-incorporated ZnO films deposited by reactive RF magnetron sputtering. *Journal of the Electrochemical Society*, *154*(9), B956.

[3] Al-Ashouri, A., Köhnen, E., Li, B., Magomedov, A., Hempel, H., Caprioglio, P., ... & Albrecht, S. (2020). Monolithic perovskite/silicon tandem solar cell with> 29% efficiency by enhanced hole extraction. *Science*, *370*(6522), 1300-1309.

[4] Aldibaja, F. K., Badia, L., Mas-Marzá, E., Sánchez, R. S., Barea, E. M., & Mora-Sero, I. (2015). Effect of different lead precursors on perovskite solar cell performance and stability. *Journal of Materials Chemistry A*, *3*(17), 9194-9200.

[5] Chen, H., Teale, S., Chen, B., Hou, Y., Grater, L., Zhu, T., ... & Sargent, E. H. (2022). Quantum-size-tuned heterostructures enable efficient and stable inverted perovskite solar cells. *Nature Photonics*, *16*(5), 352-358.

[6] Guarnera, S., Abate, A., Zhang, W., Foster, J. M., Richardson, G., Petrozza, A., & Snaith, H. J. (2015). Improving the long-term stability of perovskite solar cells with a porous Al_2O_3 buffer layer. *The journal of physical chemistry letters*, *6*(3), 432-437.

[7] Kim, H. J., Kim, U., Kim, T. H., Mun, H. S., Jeon, B. G., Hong, K. T., ... & Char, K. (2012). High mobility in a stable transparent perovskite oxide. *Applied Physics Express*, *5*(6), 061102.

[8] Lee, M. M., Teuscher, J., Miyasaka, T., Murakami, T. N., & Snaith, H. J. (2012). Efficient hybrid solar cells based on meso-superstructured organometal halide perovskites. *Science*, *338*(6107), 643-647.

[9] Niu, G., Guo, X., & Wang, L. (2015). Review of recent progress in chemical stability of perovskite solar cells. *Journal of Materials Chemistry A*, *3*(17), 8970-8980.

[10] Noh, J. H., Im, S. H., Heo, J. H., Mandal, T. N., & Seok, S. I. (2013). Chemical management for colorful, efficient, and stable inorganic–organic hybrid nanostructured solar cells. *Nano letters*, *13*(4), 1764-1769.

[11] Pandey, M., Hamal, D., Basnet, B., & Kafle, B. (2022). Synthesis and optical characterization of perovskite layer for solar cell application. *arXiv preprint arXiv:2211.13410*.

[12] Parashar, M., Singh, R., & Shukla, V. K. (2021). Fabrication of perovskite solar cells in ambient conditions. *Materials today: proceedings*, *34*, 654-657.

[13] Park, N. G., & Zhu, K. (2020). Scalable fabrication and coating methods for perovskite solar cells and solar modules. *Nature Reviews Materials*, *5*(5), 333-350.

[14] Pendyala, N. K., Magdassi, S., & Etgar, L. (2021). Fabrication of perovskite solar cells with digital control of transparency by inkjet printing. *ACS Applied Materials & Interfaces*, *13*(26), 30524-30532.

[15] Song, J., Bian, J., Zheng, E., Wang, X. F., Tian, W., & Miyasaka, T. (2015). Efficient and environmentally stable perovskite solar cells based on ZnO electron collection layer. *Chemistry Letters*, *44*(5), 610-612.

[16] Stranks, S. D., Eperon, G. E., Grancini, G., Menelaou, C., Alcocer, M. J., Leijtens, T., ... & Snaith, H. J. (2013). Electron-hole diffusion lengths exceeding 1 micrometer in an organometal trihalide perovskite absorber. *Science*, *342*(6156), 341-344.

[17] Sulistianto, J., Purnamaningsih, R. W., & Poespawati, N. R. (2019, April). Optimization of rotation speed for CuSCN hole transport layer in perovskite solar cell using spin coating. In *Journal of Physics: Conference Series* (1195, 1, 012025). IOP Publishing.

[18] Takahashi, S., Hotta, S., Watanabe, A., Idota, N., Matsukawa, K., & Sugahara, Y. (2017). Modification of TiO2 nanoparticles with oleyl phosphate via phase transfer in the toluene–water system and application of modified nanoparticles to cyclo-olefin-polymer-based organic–inorganic hybrid films exhibiting high refractive indices. *ACS Applied Materials & Interfaces*, *9*(2), 1907-1912.

[19] Ullah, W., Aziz, T., Ullah, B., Jamil, M. I., Das, S. K., Ullah, R., ... & Raheel, M. (2021). Hybrid material for the fabrication of electron transport layer in perovskite solar cell. *Polymer Bulletin*, 1-23.